

IAC-18-A6.2.8

EFFECTS OF PASSIVE DE-ORBITING THROUGH DRAG AND SOLAR SAILS AND ELECTRODYNAMIC TETHERS ON THE SPACE DEBRIS ENVIRONMENT

**Camilla Colombo¹, Alessandro Rossi², Florio Dalla Vedova³, Alessandro Francesconi⁴,
Claudio Bombardelli⁵, Mirko Trisolini¹, Juan Luis Gonzalo¹, Pierluigi Di Lizia¹,
Cinzia Giacomuzzo⁴, Shaker Bayajid Khan⁴, Ricardo Garcia-Pelayo⁵,
Vitali Braun⁶, Benjamin Bastida Virgili⁶, Holger Krag⁶**

¹ Politecnico di Milano, Dep. of Aerospace Science and Technology, Milano, Italy; camilla.colombo@polimi.it

² IFAC-CNR, Sesto Fiorentino, Italy; a.rossi@ifac.cnr.it

³ LuxSpace, Luxembourg; dallavedova@luxspace.lu

⁴ CISAS “G. Colombo” University of Padova; alessandro.francesconi@unipd.it

⁵ Universidad Politécnica de Madrid; claudio.bombardelli@upm.es

⁶ European Space Agency, ESOC, Darmstadt, Germany; vitali.braun@esa.int

This paper assesses the net effect on the long-term sustainability of the space debris environment by answering the following questions: which sail or tether size do we need for deorbiting, is that achievable with current technologies? How does the cumulative collision risk scale with the sail size, and deorbiting time? How can we model a collision involving large appendages? What happens to the space debris environment when using sails or tethers massively? Can we perform collision avoidance manoeuvres in this case?

I. INTRODUCTION

Solar and drag sailing and electrodynamic tethers have been proposed as passive end-of-life deorbiting methods [1][2][3][4], and technological demonstrators are under development [5][6]. In the drag dominated regime the required area-to-mass-ratio for deorbiting a sail spacecraft is primarily dependant on the semi-major axis, growing exponentially with increasing altitude. In the solar radiation pressure dominated regime, the required area-to-mass ratio strongly depends on both semi-major axis and inclination of the initial orbit. The deorbiting phase, at least in the first phase, is achieved on an elliptical orbit, not a circular orbit like in the case of drag sail with inward deorbiting. Another technology for end-of-life satellite deorbiting is represented by electrodynamic tethers. In general, increasing the cable length as well as its cross section increases the deorbiting force.

During deorbiting the satellite passes through the debris environment. The cumulative collision risk can be quantified as a function of the collisional cross-section present in orbit and the time of exposure of this cross-section to the flux of debris present in the environment [7]. The objective of this study, funded by the European Space Agency, is to understand the net effect of using de-orbiting technologies like sails or tethers over the future debris population around the Earth. Indeed, the increased cross sectional area will decrease the deorbiting time, however they will increase the collision risk over the deorbiting phase with respect to a standard satellite. We assess the collisions risk of deorbiting satellites using these deorbiting techniques, and the consequence of such a collision in terms of global effects onto the whole debris population. To do that fragmentation models have been devised to define when a catastrophic collision will take place and to characterise the following fragments

distribution [8]. Long-term simulation of the whole space object population environment are used to evaluate the net effect of using these strategies by means of the definition of an environmental index. Finally, the effort in terms of collision avoidance manoeuvre by conventional spacecraft is assessed and methods for sails and tether to avoid small fragments with low-push manoeuvres or attitude control are investigated.

This paper will answer to the following questions:

1. Which sail size or tether length do we need for deorbiting, is that achievable?
2. How does the cumulative collision risk scale?
3. How can we model a collision involving large appendages?
4. What happens to the space debris environment?
5. Can we perform collision avoidance manoeuvres in this case?

This work's final goal (whose study logic is presented in Fig. 1) is to assess what is the net effect on the space debris environment and its long-term sustainability.

The paper is organised as follows: Section II describes the results of some debris reference long term scenarios. Section III summarises the fragmentation model devised in this study which is used for the subsequent simulations. Section IV is dedicated to the environmental effects of solar and drag sails. First the sail requirements for a given orbit are derived and its size is compared with current technological limits. Simulations involving sails are then presented together with their results. A separate paragraph (Section V) is dedicated to a sensitivity analysis of the cumulative collision probability during a sail re-entry against the spacecraft mass, the deorbiting time and the initial orbit. Section VI presents the design of deorbiting with electrodynamic tether and the long-term simulations. An analysis on the design of collision avoidance manoeuvres for close approaches where sails are involved is presented in Section VII. Finally, some conclusions are drawn in Section VIII.

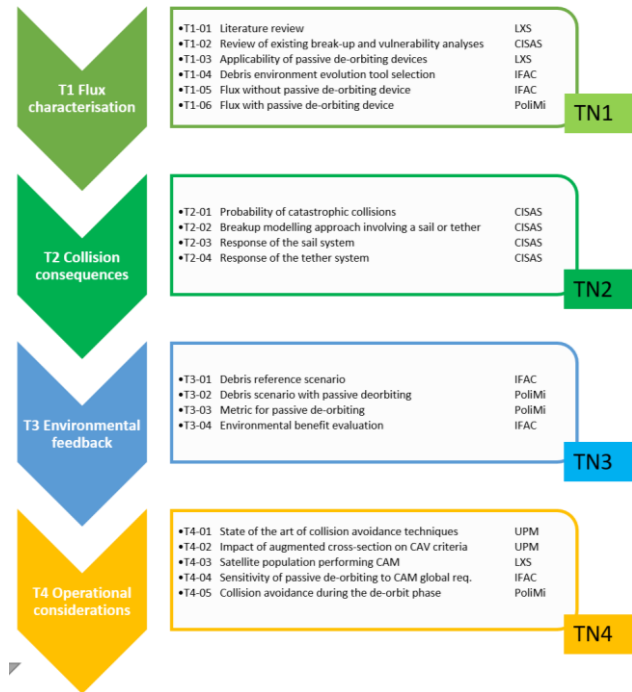


Fig. 1. Study logic.

II. DEBRIS REFERENCE SCENARIO

Five scenarios were devised where no use is made of passive de-orbiting devices such as sails or tethers. They provide different reference background long term evolutions to be compared with the cases where sails and tethers are used for deorbiting. Each scenario is simulated with at least a minimum of 50 Monte Carlo runs with the SDM code [9]. The main characteristics of the reference scenarios are reported below and summarised in Tab. 1. Note that, in some test cases, an updated launch traffic was used considering the spacecraft launched in the LEO Protected Region of mass less than 1000 kg within [01/01/2010; 31/12/2016]. A table containing mainly orbital parameters of all these spacecraft has been assembled from different sources:

1. LuxSpace (LXS) database on launched satellites
2. Union of Concerned Scientist (UCS) Satellite Database, dated 09-01-2017
3. ESA data provided to the project through extracts of DISCOS.

Tab. 1. Reference simulation set-up.

Case	Launch	Compliance to Post Mission Disposal (PDM) 25 year	Collision avoidance manoeuvre probability of success	Simulation time span [years]	Large constellation
REF-01	Business as usual (IADC)	60%	90%	100	no
REF-02	Business as usual (IADC)	90%	90%	100	no
REF-03	Business as usual (IADC) + launch traffic 2010-2016	90%	90%	100	no
REF-04	Business as usual (IADC) + launch traffic 2010-2016	60%	90%	200	yes
REF-05	Business as usual (IADC) + launch traffic 2010-2016	90%	90%	200	yes

Fig. 2 shows the effective number of objects larger than 10 cm in LEO in the five reference cases.

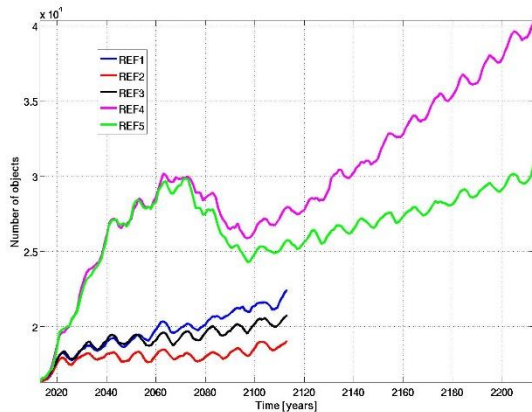


Fig. 2. Number of objects in LEO in the 5 reference scenarios.

Concentrating first in the cases without the large constellation, we note that the lowest number of objects is encountered in the REF-02 case (red line) where the launch traffic is lower and the compliance to the disposal rules is at 90%. The REF-01 case (blue line) is higher than REF-

02 due to the lower compliance to the disposal rule. In between lies the REF-03 case (black line). The outcome is significantly higher than in the REF-02 case due to the use of the increased launch traffic.

The REF-04 and REF-05 cases display the typical pace of the large constellation cases. Of course, the lower number of objects in the REF-05 case is related again to the increased compliance level with respect to the REF-04 case. It is worth stressing that in the cases under exam here an increased growth of the population after the end of the constellation lifetime, with respect to the standard constellation scenarios simulated in the previous Inter Agency Debris Committee studies, is observed. This is due to the fact that a residual number of explosions is assumed here and, mainly, to the significant increase in the background traffic that is interacting with the failed stranded constellation satellites.

III. FRAGMENTATION MODEL

This section summarises how a collision involving large appendices can be modelled. For a more detailed explanation the reader should refer to reference [8]. In this study six independent collision scenarios were considered as summarised in Tab. 2. For each of them different failure modes were described depending on specific impactor/target properties. Failure equations and collisional cross sectional areas were derived for all these scenarios. The risk assessment methodology first identifies the failure probability. For each of the elements of a sail or tether system, the number of critical impacts per unit time \dot{n}_{el} is computed as

$$\dot{n}_{el} = \int_{d_{crit,el}}^{\delta_{\infty}} \frac{\partial F}{\partial \delta} CSA_{el} d\delta$$

where F is the cumulative debris flux and δ is the debris diameter. The critical debris size $d_{crit,el}$ is the equivalent diameter (or characteristic length) of the smallest object which makes the element fail. The collisional cross sectional area CSA_{el} is the geometric cross section of the element, properly augmented to account for the impactor size as can be seen from Fig. 3.

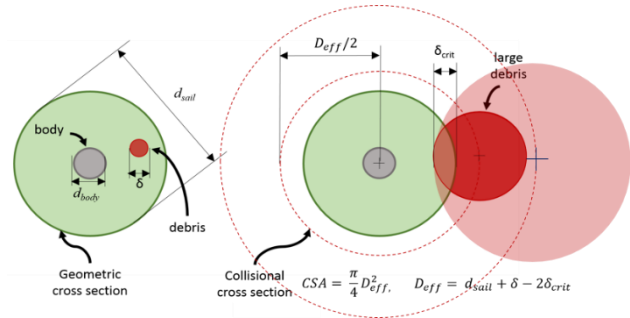


Fig. 3. Geometric (left) and Collisional (right) cross sectional areas for a circular sail membrane.

Tab. 2. List of possible collision scenarios.

Target	ID	Impactor	Comment
Spacecraft	SC1	Debris	Possible failure: spacecraft break-up (impact pressure concentrated on the contact point). Collision consequences can be modelled using the NASA SBM.
	SC3	Sail membrane	Possible failure: spacecraft break-up. Collision consequences may be different from SC1 (soft impactor, impact pressure is distributed over a large contact area).
	SC4	Boom	Possible failure: spacecraft break-up. Collision consequences may be different from SC1 and SC3, since the impact pressure is distributed over the contact line.
Sail- membrane	SM1	Debris	Possible failure: sail system loss of function. Evaluation of damage extension to sail is requested in function of the impactor properties.
Boom	B1	Debris	Possible failure: sail system loss of function due to boom cut-off.
Tether	T1	Debris	Possible failure: tether system loss of function.

The approach to break-up will be explained in the next section. The NASA Standard Break-up Model (SBM) is the starting point for fragments distributions [10]. The reason for this choice is that this is the only model founded on a credible empirical dataset. Moreover, it is widely

employed by the international debris community. However, the NASA SBM does not consider impacts involving soft objects (such as sails and tethers), neither glancing impacts, characterized by the partial overlap of colliding objects.

Two main assumptions are made in this study:

1. If any of the elements of a sail/tether system hits a spacecraft body, the NASA SBM is applied with impactor mass limited to that of its overlap with the target;
2. If any of the elements of a sail/tether system is hit by another object, a “geometric” approach is used: tethers, booms and sail membranes are cut in two pieces with negligible production of additional fragments of significant characteristic length.

Hydrocode simulations with Ansys-Autodyn have been used to evaluate the assumptions on which the proposed break-up modelling approach is based. This is necessary because available fragmentation models refer only to the impact damage caused to intact satellites by “solid” debris; “lightweight” and “soft” impactors are not considered. For each variable of interest, concurrent simulations have been run with similar/same parameters with exception of the one under investigation. In this way it has been possible to get qualitative information from the comparison of characteristic length distributions, assuming that the simulation bias is equal in concurrent cases. In other words the output sensitivity to the variation of some parameters has been investigated even though the simulations results may be uncertain.

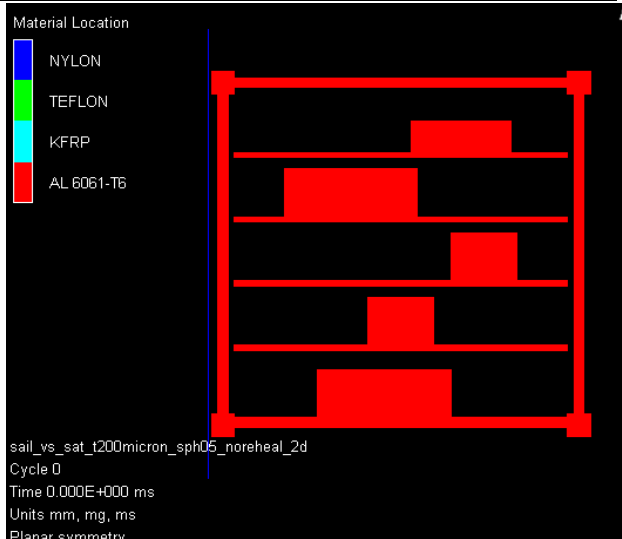
An example of a numerical simulation performed for a 1U-CubeSat target which is impacted by a sail is summarised in Tab. 3. This case aims at investigating the response of spacecraft to collisions with thin, lightweight and/or soft impactors such as booms and sail membranes. In fact, it might be thought that, because of their poor strength compared to compact debris, such impactors could be destroyed before initiating catastrophic break-up of the target, even if the impact energy (and hence EMR value) exceeds the 40 J/g threshold. If this is confirmed, the application of NASA SBM to collisions with sail membranes and booms may be considerably conservative thus leading to an overestimation of the risk posed by these de-orbiting devices. It is worth to notice that membrane thickness in this test case was set to 200 µm, which is representative of areal density of rigidised balloons (conservative assumption).

A screenshot showing the fragmentation process and the characteristic length distribution is presented in Fig. 4. The characteristic length distribution is compared with the NASA SBM, that is calculated using the total mass involved in the collision excluding those fragments that reached the material failure criterion (this mass fraction is not retrievable from the simulations output, and its integral value is specified in the figures captions).

Tab. 3. A2/2 simulation setup (2D).

A2	Evaluate EMR threshold and characteristic length distribution in case of impact pressure spread on a large area instead of concentrated in a point. (Ref. to scenarios SC3, SC4)	Thin Nylon film hitting one cube face and intersecting the cube centre, <ul style="list-style-type: none"> • 2D simulation A2/2: EMR=188 J/g (Film thickness $t = 200 \mu\text{m}$, (representative of rigidised balloon impactors))
----	---	---

	Projectile	Target
Description	Nylon film hitting the centre of one cube face	1U-CubeSat with components (boxes) inside
Size	Thick.=0.2 mm	10x10 cm ²

Mass	0.04 g/m (2D sheet)	11.2 g/m (2D sheet)	 <p>Material Location</p> <ul style="list-style-type: none"> NYLON TEFLON KFRP AL 6061-T6 <p>sail_vs_sat_t200micron_sph05_noreheal_2d Cycle 0 Time 0.000E+000 ms Units mm, mg, ms Planar symmetry</p>
Material	Nylon	Al-6061-T6	
EOS	Shock	Shock	
Strength model	Von Mises	Johnson-Cook	
Failure model	Hydro, no re-heal	Johnson-Cook	
SPH size/no.	0.05 mm / 16806	0.05mm / >9E6	
Impact speed	10 km/s		
EMR	188 J/g		

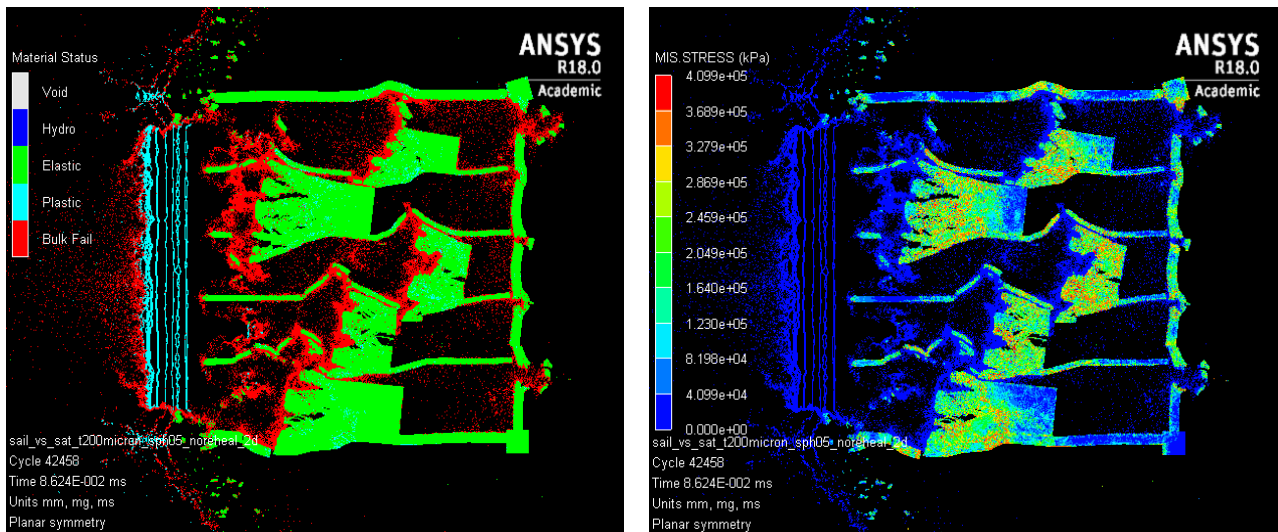


Fig. 4. A2/2 simulation at $t^*=0.086$ ms: particle status (left, failed material in red); Von Mises stress contour plot (right).

IV. DEBRIS SCENARIO WITH SOLAR AND DRAG SAILS


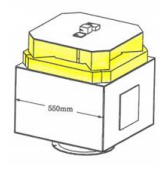
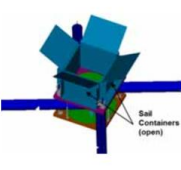
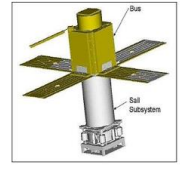

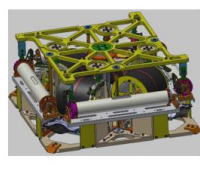
IV.I. Applicability of passive sail deorbiting devices

In order to study the applicability of passive deorbiting devices this section will present the current technological limits to the construction of sails and then will compute, for a set of initial condition, the sail area requirements.

First, the sail requirements need to be bounded by the capabilities of the current technologies, in other words: *what are the limits of current sail technologies?*

A benchmarking exercise has been performed with several reference drag and solar sail (flown) modules and/or designs reported in Tab. 4.

Tab. 4. Reference DRS/SRS projects used for benchmarking.

					
~5000 m ² ~173 kg ~0.1515 m ³	~113.5 m ² ~14 kg ~0.0900 m ³	~400 m ² ~24 kg ~0.1553 m ³	~10 m ² < 4 kg ~0.0020 m ³	~4.25 m ² ~0.95 kg ~0.0006 m ³	~25 m ² ~19.5 kg ~0.0530 m ³
VSE (1994)	Daedalus (1997)	DLR (1999)	NanoSail-D2 (2010)	CanX-7 (2014)	ADEO (2016)

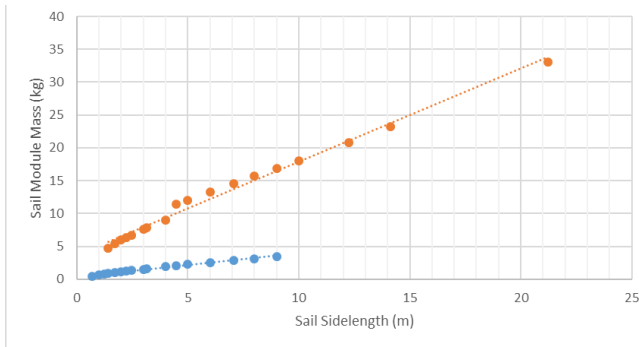


Fig. 5. Sail module masses are approximated by linear functions of the sail side lengths.

From this benchmarking exercise it resulted that, for the relatively small drag sail considered today and in the near/mid-term future (i.e. with side lengths < 25 m), the average sail areal efficiency η is equal to 92% (with the sail segments area contributing for 88% and the booms area for the other 4%) and the sail module mass is approximately a linear function of the side length (see Fig. 5). Two categories of sail module (masses) were identified, depending on the boom technologies chosen to deploy and keep the sail segments tensioned:

- For small s/c (≤ 100 kg) a mean sail module of 3 m side length was proposed for all s/c. Its features are:
 - Sail module mass: 2.4 kg
 - Ideal Sail Assembly Loading (SAL*): $2.4/9 = 0.267$ kg/m²
 - Max area (TRL 7 or 8 for sail module): ≈ 86 m².

- For larger s/c a mean sail of 5 m-side length was proposed for all. Its features are:
 - Sail module mass: 20.5 kg
 - Ideal Sail Assembly Loading (SAL*): $20.5/25 = 0.820$ kg/m²
 - Max area (TRL 6 or 7 for boom): ≈ 450 m².

Fig. 6 shows in magenta line the mass of the satellite versus the maximum sail area and sail size allowed by current sail technologies. As seen from comparison with the green line it corresponds roughly to $A/m \cdot c_R = 2$ m²/kg.

The equations used for computing the maximum sail mass m_{sail} given the spacecraft mass $m_{s/c}$ are

$$m_{sail} = 2.7063 \cdot m_{s/c}^{-0.029} \text{ if } m_{s/c} \leq 100 \text{ kg and } A \leq 86 \text{ m}^2$$

$$m_{sail} = 21.671 \cdot m_{s/c}^{-0.009} \text{ if } 100 \leq m_{s/c} \leq 1000 \text{ kg and } A \leq 450 \text{ m}^2$$

corresponding to the small and large boom sail technology.

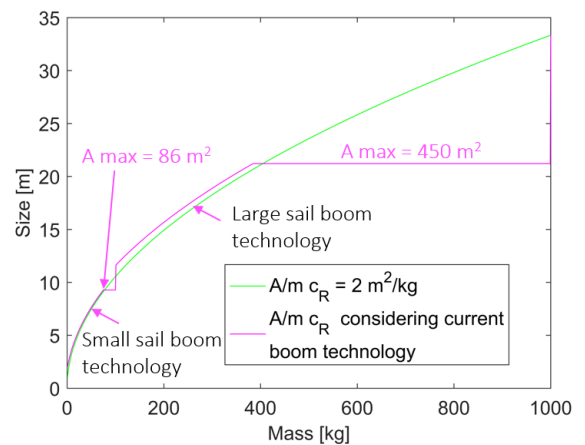


Fig. 6. Sail size technological limits.

The sail requirements were defined by setting a desired deorbiting time $T_{\text{deorbiting}}$ for the spacecraft using a solar or drag sail. As we want to define the sail requirements for many spacecraft and many initial conditions, a matrix of orbit altitudes $a - R_E$ (a being the orbit semi-major axis and R_E the mean radius of the Earth) and inclinations i was defined. This is considered to be the operational orbit where the satellite deploy a sail once the deorbiting phase is initiated.

For each initial condition and the desired deorbiting time $T_{\text{deorbiting}}$ the required drag or solar + drag sail is numerically calculated. This consist in finding the effective area-to-mass ratio to deorbit, namely A/mc_R or A/mc_D , where A is the cross area exposed to the solar radiation pressure or to drag, m is the mass of the spacecraft plus the deorbiting kit, and c_R and c_D are the reflectivity and drag coefficients respectively. For these simulation a reflectivity coefficient of 1.8 and a drag coefficient of 2.1 is used.

Given a value of the effective area-to-mass ratio and an initial orbit condition the orbit evolution is propagated with the semi-analytic propagator PlanODyn [11] considering solar radiation pressure, atmospheric drag with a Jacchia 77 exponential model with exospheric temperature of 750 K and no solar flux variation as described in Technical Note 1 [12], and the effect of zonal harmonics up to order 6. The orbit evolution is computed for a maximum time until deorbit is reached below an altitude of 70 km.

The sail requirements are computed for a desired deorbiting time $T_{\text{deorbiting}}$ of 10 years and 25 years and are represented in Fig. 7, both computed for an initial Right Ascension of the Ascending Node (RAAN) of 45 degrees. The colour bar indicates the value of A/m for deorbiting. Note that these simulations are computed for $c_R = 1$ and $c_D = 2.1$, but the results can be rescaled for any values of the reflectivity and drag coefficient in case these change. It was noted that, on such a long deorbiting time, the choice of the initial right ascension of the ascending node does not change the results. Note that, the matrix presented below could be extended to higher initial altitudes if the limits on the effective area-to-mass ratio are increased. For initial orbits with higher inclination and semi-major axis more complex solar sailing strategies can be used to allow deorbiting exploiting solar sail only. For example, a modulating strategy was proposed in [12], to have a monotonic decrease of the perigee radius. These are not considered in this study, which is limited to considering not-controlled (i.e., tumbling) sail. It has therefore to be noted that the A/m showed in Fig. 7 have to be considered the one for a tumbling sail, therefore representing the averaged cross sectional area of the sail. So in reality the sail dimension will be smaller.

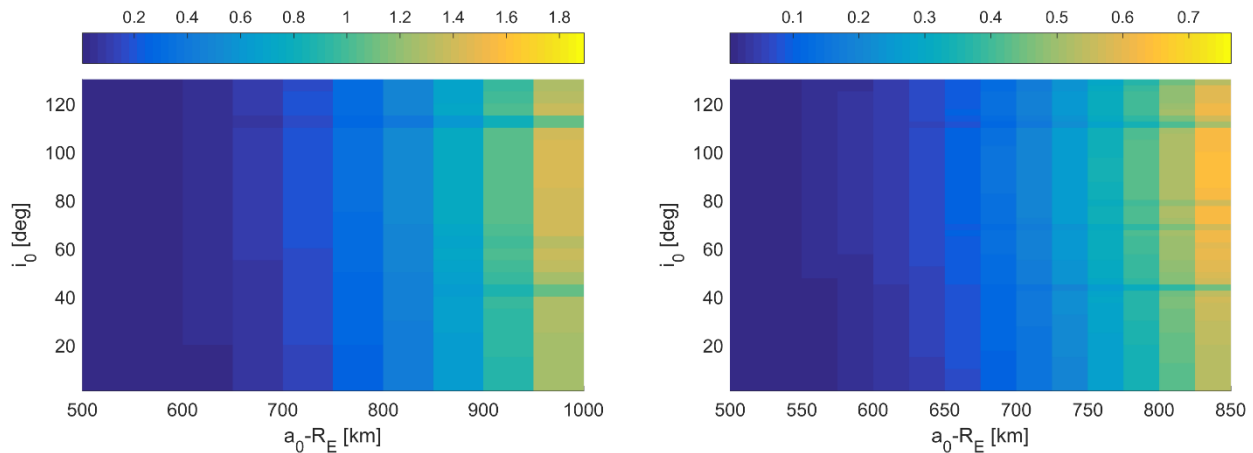


Fig. 7. Area to mass requirement for deorbiting in (a) 10 years and (b) 25 years. Initial eccentricity 0.001 and initial right ascension of the ascending node 45 deg.

IV.II. Simulations plan for sail deorbiting

Comparing with the reference scenarios described in Section II, four cases where the sails are used to deorbit the

satellites at the end-of-life were simulated. A summary of the parameters of the four sail scenarios is reported in Tab. 5. All the four sail scenarios were simulated with at least 50 Monte Carlo runs.

Tab. 5. Sail scenario set-up.

Case	Set-up	s/c using the sail	Percentage of s/c using the sail	Sail dimension for deorbiting in	Large constellation	Sail/Balloon percentage	Simulation time [years]
SAIL-01	REF-04	< 1000 kg	50% below 800 km 100% above 800 km	25 years	Do not use the sail	90% sail 10% balloon	100
SAIL-02	REF-04	< 1000 kg	100% below 800 km 100% above 800 km	25 years	Do not use the sail	90% sail 10% balloon	200
SAIL-03	REF-04	< 1000 kg	100% below 800 km 100% above 800 km	10 years	Do not use the sail	90% sail 10% balloon	100
SAIL-04	REF-05	< 1000 kg	100% below 800 km 100% above 800 km	10 years	Do not use the sail	90% sail 10% balloon	200

IV.III. Sail cases results

Fig. 8 shows the effective number of objects in LEO in the first three sail cases SAIL-01 to SAIL-03, compared to the background case REF-04, where no sails were used.

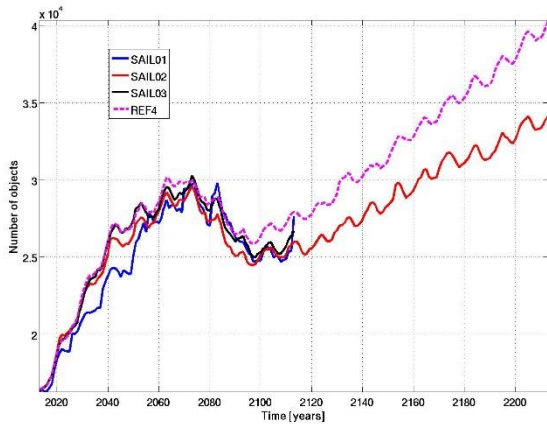


Fig. 8. Effective number of objects larger than 10 cm in LEO for the SAIL-01 to 03 scenarios, compared with the REF-04 case (dashed magenta line).

As example Fig. 9 shows the breakdown of the population in the scenario SAIL-04 in terms of different components. An additional line (in cyan) shows the number of sails present in space. It can be seen how this number stabilises, after the initial growth, thanks to the balance between new opened sails and re-entering ones. Note that this number also includes stranded sails (i.e., sails damaged by collisions – see later) and sails that, as mentioned above, are staying in space for a time span longer than the one detailed in the scenario definition, due to technological limitations in its actual size.

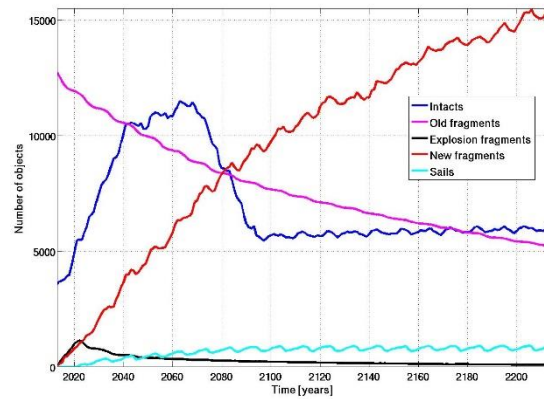


Fig. 9. Breakdown of the number of objects in LEO in the SAIL-04 scenario.

Fig. 10 shows the cumulative number of catastrophic and non-catastrophic collisions for the four sail cases, compared with the two underlying reference scenarios. First it can be noticed how, unlike the plots showing the number of objects, a significantly increased collision activity is observed in the scenarios where the sails are used. This is clearly related to the increased cross sectional area in orbit. Nonetheless, the increased number of collisions involving the sails is not generating large fragments clouds and thus is not significantly contributing to the overall debris population. To highlight the different collisional processes happening in the presence of the sails, it is worth noting, from the right panel of Fig. 10 how, differently from the reference scenarios, the number of non-catastrophic collisions exceeds the number of catastrophic ones in the sail cases.

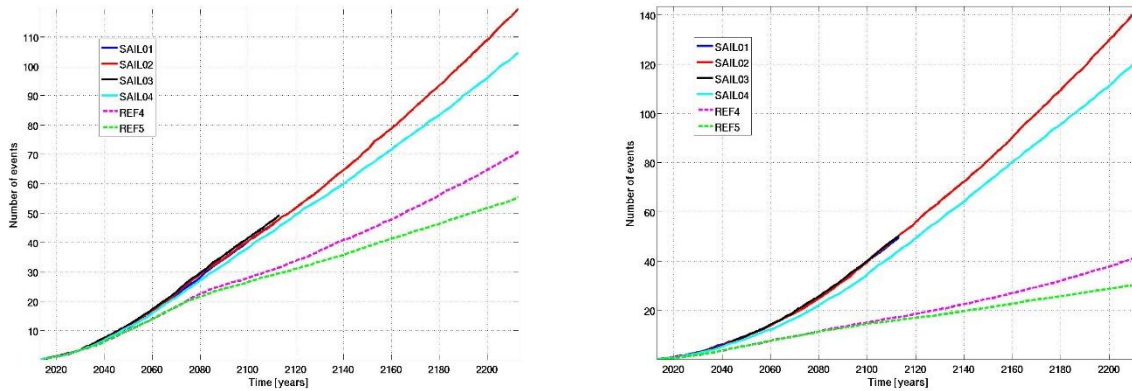


Fig. 10. Cumulative number of (a) catastrophic and (b) non-catastrophic collisions in the four sail cases, compared to the REF-04 and REF-05 scenarios.

V. COLLISION RISK: HOW DOES THE CUMULATIVE COLLISION RISK SCALE?

The possibility to use solar/drag sails as deorbiting device for satellites up to 1000 kg has been investigated in the present study. Both the requirements concerning the deorbiting time of the satellite after decommissioning (25-year rule) and the actual manufacturing limitations of the sails have been considered in order to properly assess the efficacy of such solutions. However, the deployment of a sail considerably increases the cross-sectional area of a satellite; consequently, its interaction with the debris environment during the deorbiting phase has been analysed in Section IV. In fact, the increased cross-section tends to generate a higher probability of collision for the ensemble constituted by the spacecraft body and the sail. At the same time, it is also important to consider that the probability of collision is also influenced by the environmental density of the debris in a specific region (which is mainly a function of the altitude and inclination of the orbit), and by the time spent by the satellite in such region. As different sizes of sails and the natural perturbation that they exploit, depending on whether they are drag or solar sails, generate different deorbiting times, it is interesting to study the effect that different sail sizes have on the cumulative collision probability of a spacecraft. In fact, a larger sail

has a larger debris collection area; however, it also enables shorter deorbiting times, thus limiting the exposure of the satellite to the debris environment. In addition, the specificity of the orbital perturbations influencing the motion of the satellite around the Earth, for specific combinations of initial orbital conditions and sail area, may enhance the deorbiting capability of the sail, drastically reducing the time needed for deorbiting. This is also reflected onto the collision probability, as the combination of cross-sectional area and time spent deorbiting may be particularly favourable.

In this paragraph the sensitivity of the collision probability as a function of the initial orbit, the sail size, the deorbiting time, and the mass of the satellite is studied. For all the initial orbits in the grid in semi-major axis and inclination used in Section IV, a deorbiting trajectory and the corresponding sail requirement are computed specifying the desired decay time of 5, 10, 15, and 25 years. The cumulative penetration probability related to each one of the deorbiting trajectories generated was computed through the ESA software package MASTER-2009 [14].

While the collision probability shows a quasi-linear increase with the spacecraft mass, as sail cross sectional area increases with mass, the sensitivity to the initial orbit is more interesting.

Fig. 11 shows the collision probability for a 100 kg spacecraft with a decay time of 25 years. At lower altitudes (up to 1000 km) is noticeable a regular behaviour, with a greater collision probability for spacecraft starting at higher altitudes and thus passing through the most populated debris regions. At higher altitudes the deorbiting is driven by solar radiation pressure, along an elliptical path, therefore the collision probability is lower.

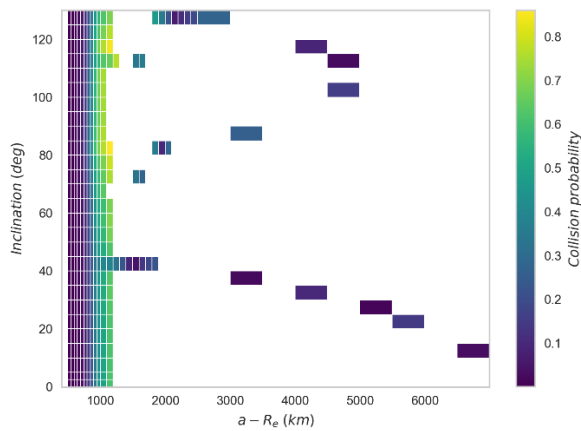


Fig. 11. Collision probability for a 100 kg spacecraft with a decay time of 25 years.

Fig. 12 shows instead the ratio between the number of impacts for a 25 years decay orbit and a 5 years decay orbit, considering a minimum debris particle of 1 mm.

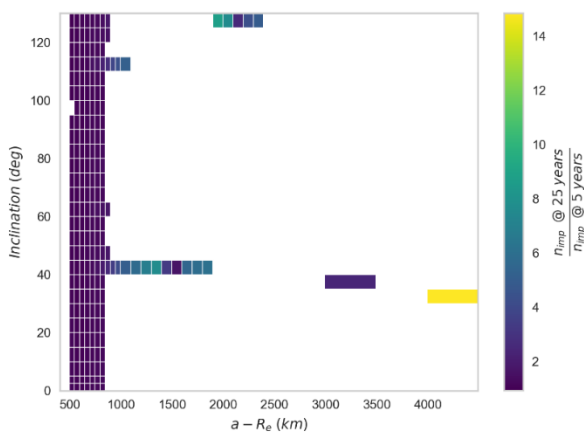


Fig. 12. Ratio between the number of impacts for a 25 years decay orbit and a 5 years decay orbit, minimum debris particle: 1 mm.

For drag driven deorbit the ratio is around 1 (i.e. linear relationship), while for deorbiting driven by solar radiation pressure the ratio is higher than 1, indicating that a shorter deorbiting time with a larger sail is better than longer deorbiting with a smaller sail.

VI. DEBRIS SCENARIO WITH ELECTRODYNAMIC TETHERS

VII. Applicability of electrodynamic tethers

To have a realistic Electro Dynamic Tether (EDT)-assisted deorbiting scenario in LEO it is important to understand the domain of applicability of EDTs and the relation between their deorbiting performance and design parameters. In addition, in order to provide a simple and practicable interface with the space debris SDM code, it is paramount to develop suitable analytical surrogate models providing the evolution of the tethered debris ephemerides given all the fundamental input design parameters:

- **Maximum lifetime:** EDTs work best for short deorbiting times, ideally a few months, so that the degradation of their critical components can be reduced to a minimum. Taking into account current technology, EDTs should not be considered for very long (> 3 years) deorbiting, as that would exceed the predicted lifetime of the hollow cathode electron emitter [4].
- **Micro- and nano-satellite applicability limits:** EDTs are particularly suitable to deorbiting medium (100 to 1000 kg) satellites, where they can be packed and integrated without compromising the spacecraft functionalities. Below a certain size (say, 20 kg), a scalability issue appears that complicates their applicability [14]. This is due to two main facts. The first is that very short (<100 m) tethers are very inefficient as the electric potential across the full length is barely enough to compensate the potential drop of the electron emitter. The second is that the latter cannot be easily miniaturised (again, assuming

current technology). As a result, the whole EDT system, including the conductive tape, the electron emitter and the required deployment elements cannot easily fit on a very small satellite.

- Maximum tether length: Extremely long (> 10 km) tethers should be avoided due to deployment complexity and micrometeoroids survivability issues [18].
- Maximum orbit eccentricity: EDTs behaviour for eccentric orbits (i.e. $e > 0.01$) is very complex. If not continuously controlled their attitude motion would

become unstable leading to a spin-mode transition [16].

- Maximum orbit altitude: Due to the insufficient plasma electron density and magnetic field magnitude, EDTs do not work well beyond 2000 km altitude [17].

Tab. 6 shows the deorbiting time for different initial inclination and orbit altitudes simulated via EDTdromo [19][20]. All the simulations considered a 2 km tape EDT with 3 cm width and a debris mass of 200 kg.

Tab. 6. Deorbiting performance (days) of a 2-km tape EDT with a 200-kg s/c.

h / / inc	5°	15°	25°	35°	45°	55°	65°	75°	85°	95°	105°
550 km	1	1	2	2	4	6	9	17	29	28	16
650 km	2	2	3	4	6	10	16	31	54	52	29
750 km	4	4	5	8	11	16	27	53	92	85	51
850 km	7	7	9	12	17	26	45	85	148	132	81
950 km	11	12	14	19	27	41	67	124	235	216	122
1050 km	17	18	21	29	40	59	96	187	308	297	178
1150 km	24	26	31	41	57	82	130	258	388	375	247
1250 km	34	37	43	57	76	107	180	321	485	468	306
1350 km	45	49	58	74	97	140	238	395	625	605	369
1450 km	58	62	72	92	124	182	290	481	762	739	450
1550 km	72	77	89	115	154	233	345	600	973	934	561
1650 km	88	95	109	140	197	278	410	714	1195	1162	693
1750 km	107	115	132	175	238	321	479	861	1487	1454	850
1850 km	127	138	159	213	277	373	569	1064	2009	1933	1044

Tab. 7. Tether scenario set-up.

Case	Set-up	s/c using	s/c orbit from where	Percentage of s/c	Tether dimension for	Large constellation	Simulation time [years]

		the tether	to use a tether	using the tether	deorbiting in		
TETHER-01	REF-04	< 1000 kg	circular orbits with $h < 2000$ km	100%	3 years	Do not use the tether	200
TETHER-02	REF-04	< 1000 kg	circular orbits with $h < 2000$ km	50%	3 years	Do not use the tether	100

VI.II. Simulations plan for tether deorbiting

Similarly to the sail cases, two scenarios where EDTs are used to deorbit the spacecraft at the end-of-life were simulated (see

Tab. 7). All the EDT scenarios were simulated with at least 50 Monte Carlo runs.

VI.III. Electrodynamic tether cases results

Fig. 13 shows the effective number of objects in LEO in the tether cases TETHER-01 and TETHER-02, compared to the background case REF-04, where no tethers were used.

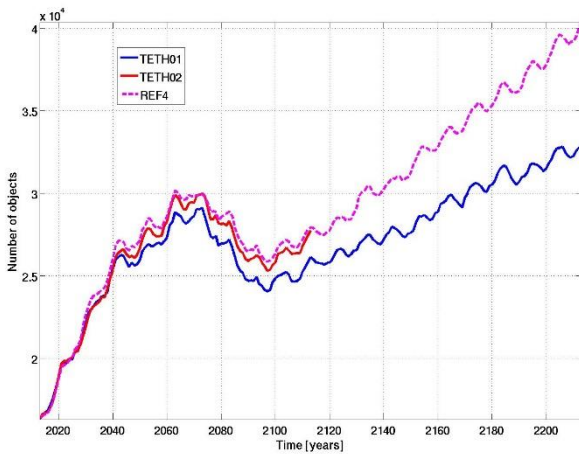


Fig. 13. Effective number of objects larger than 10 cm in LEO for the two tether scenarios.

In the long term scenario TETHER-01, where all the satellites, within the limits detailed above, are using a tether to de-orbit in 3 years, a significant reduction of almost 20% in the number of objects in LEO is observed after 200 years. Once again it has to be stressed that the comparison is made between a scenario (REF-04) where

only 60% of the satellites are compliant to the 25-year with a scenario (TETHER-01) where 100% of the satellites are de-orbited in 3 years.

VII. COLLISION AVOIDANCE MANOEUVRES INVOLVING SAILS

The results presented so far show that the larger cross section of sails may increase collision risk. And even if many of these collisions are not catastrophic, they can reduce the effectiveness of the sail or render it useless. Therefore, the design of collision avoidance manoeuvres (CAMs) for close approaches (CAs) involving sails has been studied [21], treating the sail either as the debris or the manoeuvring spacecraft.

For the case where the sail is the debris, an analytic method for designing impulsive CAMs has been proposed using Gauss planetary equations and a relative motion formulation [21]. Two strategies are compared, either maximizing miss distance in the b-plane or minimizing collision probability. Representing dynamics in the b-plane of the CA provides greater insight on the dynamics, separating the effects along the time (pushing related) and geometry (MOID related) axis. As an example, Fig. 14 shows a test case where the minimum collision probability and maximum miss distance CAMs yield a very different collision probability for a very similar miss distance.

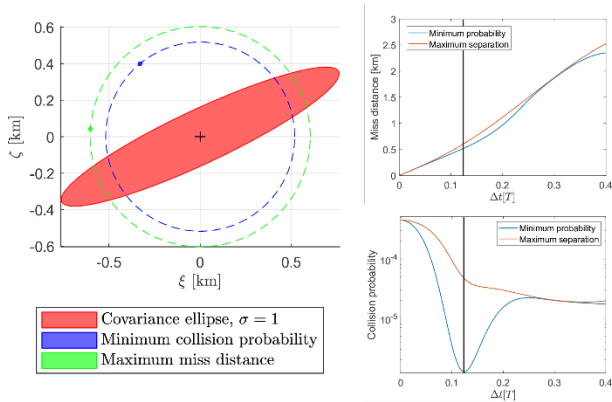


Fig. 14 b-plane representation of min. collision probability and max. miss distance CAMs, for a lead time of 0.1241 periods of the spacecraft

On the other hand, a simple strategy has been proposed for CAMs by sails in the drag dominated scenario. Mainly, the sail is set parallel to the main force to achieve a phasing effect by removing drag. Results for several area-to-mass ratios and lead times are given in Fig. 15, using real data from a conjunction data message provided by ESA. It is checked that this strategy is effective for sufficiently large CAM lead times, which depend on the area-to-mass ratio of the sail. Interestingly, there can be an initial increase in collision probability or decrease in miss distance, depending on the geometry of the CA in the b-plane.

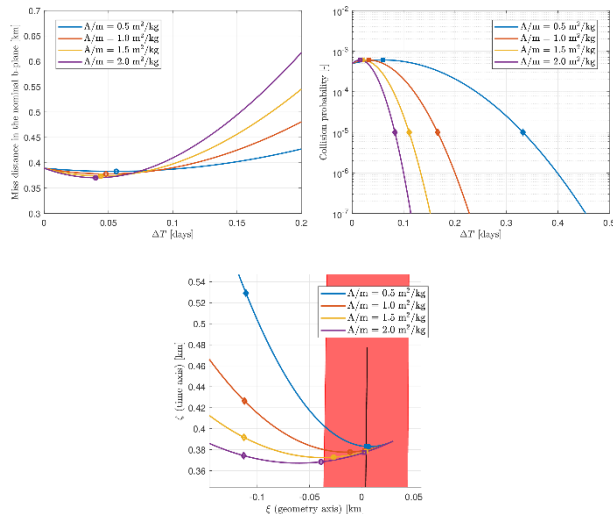


Fig. 15 Sail CAMs for different area-to-mass ratios and a 2-days warning CDM. Circles represent min. miss distance, squares max. collision probability, and diamonds a 10^{-5} collision probability.

VIII. CONCLUSION

This paper assesses the applicability of passive de-orbit devices to the disposal phase of satellites, and its effect in the s/c population. The analysis focuses on satellites with mass below 1000 kg, to reflect the fact that objects with larger mass tend to have a propulsion system and thus are unlikely to require passive de-orbit means. The database of launched satellites between 2010 and 2016 was analysed considering also the distribution of spacecraft in different regions of spaces and mass classes. The interdependency of the three criteria that characterise the deorbiting, namely area-to-mass (sail) or length-to-mass (EDT) requirement, deorbiting time, and collision probability is analysed. Long term simulations with SDM are performed to study the net effects of these deorbiting devices on the long-term evolution of the space debris population. In general, even if the number of collisions is higher, the total number of space debris fragments on the long term is lower as these collisions do not generate large fragments clouds and thus are not significantly contributing to the overall debris population. The last part of this study, tackles the question: can we perform collision avoidance manoeuvres in the case sails are used?

IX. ACKNOWLEDGMENTS

The work performed for this paper is funded through the European Space Agency contract 4000119560/17/F/MOS.

X. REFERENCES

- [1] Janovsky, R. et al., "End-of-Life de-Orbiting Strategies for Satellites", *54th International Astronautical Congress*
- [2] Lücking, C., Colombo, C. and McInnes, C. R., "Solar Radiation Pressure-Augmented Deorbiting: Passive End-of-Life Disposal from High Altitude Orbits," *Journal of Spacecraft and Rockets*, Vol. 50, No. 6, 2013, pp. 1256-1267. doi: 10.2514/1.A32478.
- [3] Lücking, C., Colombo, C. and McInnes, C. R., "A Passive Satellite Deorbiting Strategy for Medium Earth Orbit Using Solar Radiation Pressure and the J_2 Effect," *Acta Astronautica*, Vol. 77, 2012, pp. 197-206. doi: 10.1016/j.actaastro.2012.03.026.
- [4] Bombardelli, C., Personal communication with team members of the FP7 project "BETs" "The Bare Electrodynamic Tethers Project".
- [5] Colombo, C., Rossi, A., Dalla Vedova, F., Braun, V., Bastida Virgili, B. and Krag, H., "Drag and Solar Sail Deorbiting: Re-Entry Time Versus Cumulative Collision Probability," Proceedings of the 68th International Astronautical Congress, Adelaide, Australia, 2017, IAC-17-A6.2.8.
- [6] LuxSpace, GNC for deployable sail de-orbit devices (ESA ITT AO/1-8007/14/NL/MH)
- [7] Klinkrad, H., *Space Debris - Models and Risk Analysis*, Springer, 2010, ISBN: 978-3-540-37674-3.
- [8] Francesconi, A., Giacomuzzo, C., Shaker Khan, B., (2017). Collision consequences for passive de-orbit devices. ESA/ESOC Contract No. 4000119560/17/F/MOS "Environmental aspects of passive de-orbiting devices". Technical Note 2, Version 2.0.
- [9] Rossi, A., Anselmo, L., Pardini, C., Jehn, R., and Valsecchi, G. B., "The new Space Debris Mitigation (SDM 4.0) long term evolution code," in Proceedings of the Fifth European Conference on Space Debris, 2009.
- [10] Krisko, P. H., "Proper Implementation of the 1998 NASA Breakup Model", *Orbital Debris Quarterly News*, Vol. 15, No. 4-5, 2011.
- [11] Colombo, C., "Planetary Orbital Dynamics (PlanODyn) suite for long term propagation in perturbed environment", 6th International Conference on Astrodynamics Tools and Techniques (ICATT), 14-17 Mar. 2016, Darmstadt.
- [12] Colombo, C., Langlois D'Estaintot, M., Dalla Vedova, F., Rossi, A., Francesconi, A., Giacomuzzo, C., Bombardelli, C., and Garcia-Pelayo, R. (2017). Flux analysis using passive de-orbiting systems. ESA/ESOC Contract No. 4000119560/17/F/MOS "Environmental aspects of passive de-orbiting devices". Technical Note 1, Version 2.0.
- [13] Colombo, C., and de Bras de Fer, T., "Assessment of passive and active solar sailing strategies for end-of-life re-entry", 67th International Astronautical Congress, Guadalajara, Mexico, IAC-16-A6.4.4.
- [14] Flegel, S., Gelhaus, J., Wiedemann, C., Vorsmann, P., Oswald, M., Stabroth, S., Klinkrad, H., and Krag, H., "The MASTER-2009 space debris environment model", Fifth European Conference on Space Debris, Vol. 672, 2009.
- [15] Sánchez-Arriaga, G., Bombardelli, C., and Chen, X., "Impact of nonideal effects on bare electrodynamic tether performance", *Journal of Propulsion and Power* 31 (3), 951-955.
- [16] Sidorenko, V.V., and Celletti, A., 2010. A "Spring-mass" model of tethered satellite systems: properties of planar periodic motions. *Celestial Mechanics and Dynamical Astronomy*, Vol. 107, pp. 1-2, pp.209-231.
- [17] van der Heide, E.J., and Kruijff, M., 2001. "Tethers and debris mitigation". *Acta Astronautica*, Vol. 48 pp. 5-12, pp.503-516.
- [18] Shaker Bayajid, K., and Sanmartin, J. R., "Survival probability of round and tape tethers against debris impact." *Journal of Spacecraft and Rockets* 50.3 (2013): 603-60.
- [19] Sanmartin, J. R., Martinez-Sanchez, M., and Ahedo, E. "Bare wire anodes for electrodynamic" tethers. *Journal of Propulsion and Power*, 9, 3 (1993), 353-360
- [20] Bombardelli, C., Pelaez, J., and Sanjurjo, M., 2010. "Asymptotic solution for the current profile of passive bare electrodynamic tethers". *Journal of propulsion and power*, 26(6), pp.1291-1304.
- [21] Gonzalo, J.L., Colombo, C., and Di Lizia, P., "Analysis and design of collision avoidance maneuvers for passive deorbiting missions", AAS/AIAA 2018 Astrodynamics Specialist Conference, Snowbird, UT, 19-23 August 2018, paper AAS 18-357.